Pertanika J. Sci. & Technol. 32 (S1): 21 - 32 (2024)

PERTANIKA JOURNALS

SCIENCE & TECHNOLOGY

Journal homepage: http://www.pertanika.upm.edu.my/

Performance Evaluation of UAV Airfoil Under Various Ground Conditions

Dhanya Prakash R Babu[1,2]*, Madhesh Devasenan[2], Ganeshan Pushpanathan[3] and Mukesh Raju[4]

[1]Department of Aeronautical Engineering, ACS College of Engineering, Bangalore 560074, India
[2]Department of Mechanical Engineering, Academy of Maritime Education and Training (AMET) Deemed to be University, Chennai 603112, India
[3]Centre for Augmented Intelligence and Design, Department of Mechanical Engineering, Sri Eshwar College of Engineering, Coimbatore 641202, India
[4]Department of Aerospace Engineering, ACS College of Engineering, Bangalore 560074, India

ABSTRACT

Investigation of ground effects on Unmanned Aerial Vehicle (UAV) are limited. The UAV's ground effect on the water surface and irregular surfaces has not been studied well. The principal objective of this research is to apply numerical solutions to investigate the flow physics and aerodynamic characteristics of selected NACA4412 airfoil for different h/c and surface roughness conditions in the ground effect scenario. The k-ω turbulence model and compressible RANS equations are solved using the Finite Volume Method (FVM). The simulated data is authenticated with the reference data and compared with the DATCOM data. The results express that the lift coefficient variations for various surface roughness are affected by the h/c proportion. The drag coefficient for various roughness has the same pattern for different ratios and almost has the same difference from high to lower values. The result shows that the DATCOM code cannot predict the aerodynamic characteristics with ground effects.

Keywords: Aerodynamic characteristics, DATCOM, ground effects, h/c ratio, roughness

ARTICLE INFO

Article history:
Received: 27 July 2023
Accepted: 17 October 2023
Published: 19 January 2024

DOI: https://doi.org/10.47836/pjst.32.S1.02

E-mail addresses:
dhanyaprakashr@gmail.com (Dhanya Prakash R Babu)
madhesh.d@ametuniv.ac.in (Madhesh Devasenan)
ganeshan.p@sece.ac.in (Ganeshan Pushpanathan)
vsmprm@gmail.com (Mukesh Raja)
*Corresponding author

INTRODUCTION

The term "ground effect" denotes the favorable influence on an aircraft wing's horizontal surfaces' lifting property when the aircraft's wing is available near the ground (Figure 1). This outcome comes from the ground's nearness changing the airflow below the surfaces. Ground Effect's ability to increase lift is primarily due to a

ISSN: 0128-7680
e-ISSN: 2231-8526

decrease in drag produced, which raises lift to drag ratio. In maximum cases, a direct rise in lift produced by the wing supplements this enhanced lift. The wing tip is where induced drag decreases, depending on wing lift. The shape of the wing tip vortex, created as an airfoil passes through the air due to the pressure underneath a wing being greater than the pressure above it, is altered when it is created near the ground. When the airflow is forced outward, vortices close to the ground become elliptical instead of circular. It raises the wing's effective aspect ratio over its geometric aspect ratio and lowers generated drag. Power, lift, and airspeed are enhanced for any specific engine.

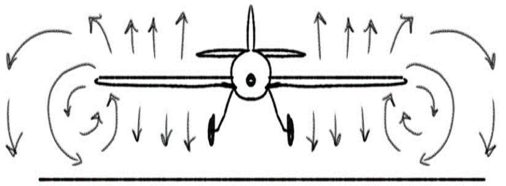

Figure 1. Ground effect

There are two types of ground effects: in-ground and out-ground. In the air downside, the airfoil can react with the ground, whereas in the out-ground effects, the air is not able to react with the ground. In the case of ground effect, less angle of attack (AOA) is needed for a given amount of lift before a wing stalls. The degree of this reduction in stalling AOA will depend on the type of airfoil used, although it may be some degree. Any decrease in a specific wing's maximum coefficient of lift in ground effect relative to that coefficient in free air will likewise influence the differential. Figure 2 illustrates the variation of stalling AOA in and out of the effect caused by the ground. It follows that for a given AOA, the wing will produce maximum lift at a lower AOA than in free air because carrying a wing into the ground improves lift. Figure 3 illustrates the pressure distribution on the wing due to ground effect.

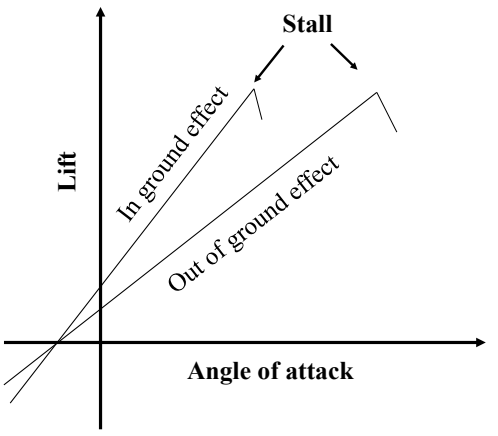

Figure 2. Ground effect in lift

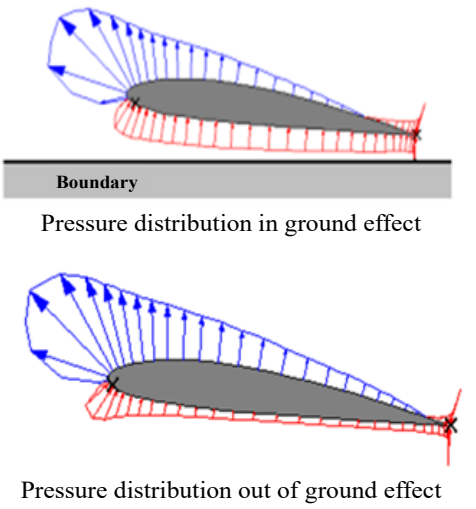

Figure 3. Pressure distribution due to ground effect

DATCOM was created in FORTRAN in 1979 and retitled by USAF. DATCOM is intended to be used for the preliminary design of an aircraft. It considers the conventional body-wing-tail configurations, which include control effectiveness for various high-lift control devices. It is the computer program to speed up the process of analyzing the existing or new design. Based on the configuration details of the design and the flight condition, it can immediately give the aerodynamic derivative of the aircraft. DATCOM calculates the static stability, high lift and control devices, and dynamic derivatives features. It also provides a trim option for determining the control deflections at subsonic Mach numbers. It has been created modularly, and the modular approach is used because it simplifies the program development.

De Divitiis (2005) proposed the analytical formulation for the force and moment calculation in the existence of ground and at an altitude. The study investigated the aerodynamic characteristics of a vehicle at an altitude and in the existence of ground effect and discussed the stability and performance characteristics of the vehicle. Then, the study validated the obtained results with the literature results and concluded that the coefficient of lift increases when h/c (ratio of height above ground to the airfoil chord) diminishes in the effect of the ground. Jamei et al. (2012) investigated the aerodynamic behavior of compound wings in ground effects. They selected NACA 6409 airfoil for the compound wing. The aerodynamic coefficients of the wing are associated with the rectangular wing for various ground clearances. They concluded that the compound wing had a high lift coefficient and a lower drag coefficient than the rectangular wing for the small ground gap.

Using CFD Simulation, Qu et al. (2014a) studied the NACA 4412 airfoil aerodynamic characteristics in dynamic ground effects. They concluded that the dynamic ground effect lift is less than the static ground effect when h/c is less than one. It is nearly equal to the static effect when h/c is between 0.5 and one and is greater than the static effect when h/c is greater than one. Using ANSYS Fluent, Qu et al. (2014b) simulated the flow around a wing in ground effects flying at an angle of attack 3° and 9° over the wavy and flat ground. They concluded that the lift, drag, and pitching moments are periodic when the wing is in the wavy ground, the aerodynamic forces are in the same pattern for the flat and wavy ground, and the aerodynamic forces increase for both angles of attack as the flight height decreases. However, the lift-to-drag ratio increases for the angle of attack of 3° while the lift-to-drag ratio rises first and then decreases for the AOA of 9°.

Roozitalab and Kharati-Koopaee (2021) investigated the Gurney flap's effect on the aerodynamic characteristics of the NACA 4412 airfoil in mutational ground effect during the launch and landing process. They concluded that during those times, the lift coefficients decrease, and the decrease in lift and increase in drag is more favorable in the landing process than the takeoff process. Gao et al. (2018) experimented with the RAE2822 airfoil's flow mechanics and aerodynamics by altering the ground clearance from the ground at

alpha sweeps of 0 to 12 degrees and Mach numbers of 0.5 to 0.8 in ground effect. The experiment concluded that in the high ground gap, lift increases by a small amount and drag increases due to the stagnation point downward movement, which decreases the strength of the shock, and in low ground clearance, the lift decreases, and the drag increases due to the presence of shock on the airfoil at the lower surface.

Page and McGuirk (2009) demonstrated the feasibility of LES CFD Methodology to represent the Harrier aircraft at touch-down. They concluded that the LES method is the appropriate tool for predicting the mean flow and unsteady oscillations, which is difficult in RANS-based CFD. Furthermore, Sharma et al. (2021) simulated the flow of wind Over the Deck and ground effects during the landing and approach of the helicopter on a ship deck and incorporated the static and finite state models. The simulation concluded that the wind over the deck induces high-frequency drifts and oscillations, more control effects are required when the wind over the deck is included for the entire helicopter, and the ground effect of static deck roll inclination causes the change in longitudinal cyclic input.

Zheng et al. (2021) studied the ditching characteristics of BWB aircraft numerically and validated the results with the high-speed ditching experimental results for 3D flat plates. The study concluded that the aircraft's proposed motion steadily diminishes until it glides on water. Further, Papadopoulos et al. (2021) presented a conceptual design of a combined box-wing and blended-wing unmanned aerial platform and studied the effect of flight without the ground effects. They concluded that the Unmanned Ground Effect Vehicle (UGEV) configuration has significant potential as a substitute for ships or seaplanes, based on its capacity to carry a higher cargo than seaplanes and transport it faster than ships.

Abney and McDaniel (2005) compared the aerodynamic results obtained from the missile DATCOM with the wind tunnel data for a high angle of attack at Mach number less than one. The prediction of normal force and longitudinal location of the center of pressure is well suited to the wind tunnel data for the AOA up to 45°. The prediction of axial force had a variance near the 30° AOA. Furthermore, Kefalas and Margaris (2018) simulated the flow field around Sonerai II LS aircraft. They concluded that the slope of the CFD lift curve is higher than that of the DATCOM lift curve. The results of digital DATCOM with those from CFD reveal that the post-stall zone has a lesser lift. The CFD data is steeper than the DATCOM.

In addition, Othman (2017) evaluated the longitudinal characteristics of an aircraft by CFD at the transonic speed and compared the results with the Wind tunnel data and DATCOM, comparing the pitching moment data. He concluded that the normal, axial, and pitching moment coefficient attained by the CFD is consistent with the wind tunnel data, but the DATCOM has a slight variation with the wind tunnel data. Moreover, the Missile DATCOM is a better prediction code for longitudinal aerodynamic coefficients for the lower angle of attack, and DATCOM prediction has nonlinear flow physics for the vortex models.

Paul et al. (2021) evaluated the prediction of aerodynamic data for four guided munitions, and the results were validated with test data. Vinayagar et al. (2022) and Ramshankar et al. (2023) studied the optimization of Crashworthiness Parameters of Thin-Walled Conoidal Structures and hybrid composites in aerospace applications. Thus, the literature review reveals that investigating the ground effect on UAVs is very limited, especially since the 'UAV's ground effect on the water surface and irregular surfaces has not been studied well.

MATERIALS AND METHODS

Methodology

To begin with, a wide literature review was done to understand the previous findings on ground effects. From the literature survey, the airfoil was selected, and the ground effects were investigated. The methodology of this work is bestowed in Figure 4. The geometry of the airfoil and mesh generation were done in ANSYS. With the fine unstructured mesh, analysis was carried out for the aerodynamic characteristics with ground effects. The CFD Analysis was carried out for different h/c ratios and surface roughness at a velocity of 30m/s. Then, the results are validated with the experimental results and compared with DATCOM data.

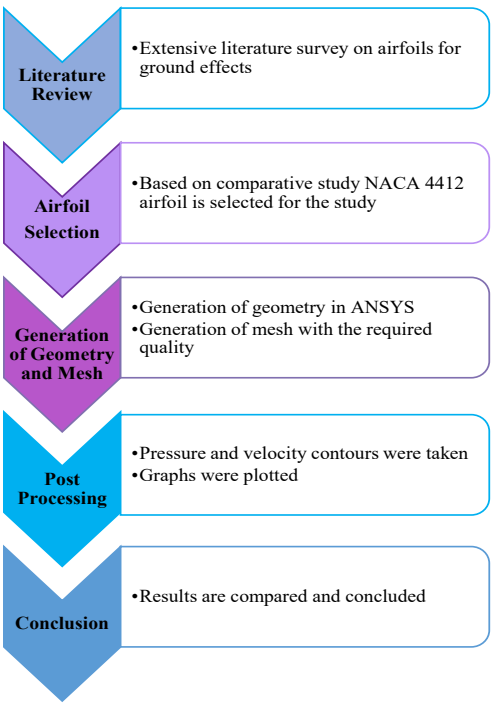

Figure 4. Methodology

Airfoil Selection and Ground Effects Investigation

The selection of the right airfoil geometry is one of the building blocks in the aerodynamic design process. Airfoil selection is based on multiple parameters such as Reynolds number, Thickness to chord ratio, Maximum coefficient of lift, and L/D ratio. Studies and research on the design of UAV wings, a few of the most common airfoils used in UAVs are NASA/Langley LS (1)-0417mod airfoil, Eppler–e 423, Selig S1223, Wortmannfx 74-cl5-140 mod, and NACA4412. Based on a comparative study, NACA4412 has shown promising characteristics that suit the requirement of a UAV wing. For further proceedings, NACA4412 will be selected as our baseline airfoil. When an aircraft glides at or below nearly half the length of the wingspan directly above the water or ground

surface, the ground effect occurs. Modern UAVs must be designed in such a way that they can take off and land on any kind of terrain. Hence, it is essential to investigate the ground effect of the UAV wing/airfoil at various ground conditions. The moving wall (ground) will be included in the simulations. Deploying flaps and spoilers may yield interesting physics when combined with ground effects.

Pre-Processing

The coordinates of NACA 4412 Airfoil are imported in ANSYS, and the domain is created. The global mesh parameters are given, and the surface mesh is generated for the domain with the minimum quality. The unstructured mesh is selected since the quality of the mesh is better than the structured mesh. Figure 5 depicts the mesh of the domain and the boundary condition.

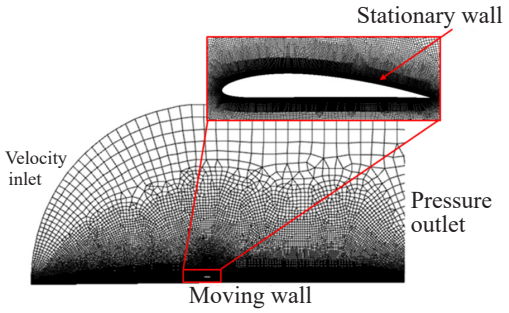

Figure 5. Surface mesh for the domain

The generated mesh has 434000 elements with 340556 nodes and a boundary layer thickness of 1 e^{-5}. The generated mesh was imported to ANSYS Fluent, and then the properties of the air were assigned. The velocity magnitude and direction were given in the boundary condition, and the reference values were given. The k-ω turbulence model equations and compressible RANS equations are used for the simulation. The governing equation for the turbulence kinetic energy is below (Jamei et al., 2012).

$$\frac{\partial(\rho k)}{\partial t} + div(\rho k U) = div\left[\frac{\mu_t}{\sigma_k} grad(k) + 2\mu_t S_{ij} \cdot S_{ij} - \rho\varepsilon\right] \quad (1)$$

$$\frac{\partial(\rho \varepsilon)}{\partial t} + div(\rho \varepsilon U) = div\left[\frac{\mu_t}{\sigma_\varepsilon} grad(\varepsilon)\right] + C_{1\varepsilon}\frac{\varepsilon}{k} 2\mu_t S_{ij} \cdot S_{ij} - C_{2\varepsilon}\rho\frac{\varepsilon^2}{k} \quad (2)$$

Where

k = turbulent kinetic energy
ρ = air density
U = Free stream velocity
S = reference area
ε = turbulent energy dissipation rate
Sij = mean rate of the deformation sensor
μ_t = air turbulent viscosity
μ = air viscosity

The analysis was performed at a speed of 30 m/s along with h/c values of 0.25, 0.5, and 1.0 and surface roughness values of 0.001, 0.005, 0.01, 0.02, 0.03, 0.04 and 0.05. The h/c is the distance ratio between the airfoil and ground to the chord length of the airfoil. The analysis was done, and the data was saved in a case and format. The results were post-processed for the analyzed data. Pressure contours and velocity contours were taken during post-processing. The C_L and C_D data obtained based on the governing equations and the data obtained are discussed later.

Post-Processing

After obtaining the results from the analysis, contour plots of pressure, velocity, temperature, and Mach number contours can be obtained from the fluent solver. In this present work, pressure contours and velocity contours were plotted. Figures 6 and 7 depict the pressure and velocity contour for the airfoil at 30 m/s, with h/c values of 1, 0.5, and 0.25 and roughness values of 0.001, 0.01, and 0.05. In Figure 6, the blue color on the upper surface of the airfoil indicates that the pressure value is low, and near the leading edge of the airfoil is red color, which has the maximum value of pressure. In Figure 7, the velocity on the airfoil's upper surface is maximum, which is red in the velocity magnitude. The velocity is zero on the surface of the airfoil. The velocity gradually increases from the surface of the airfoil to the maximum value, which the color variation can be seen in the images.

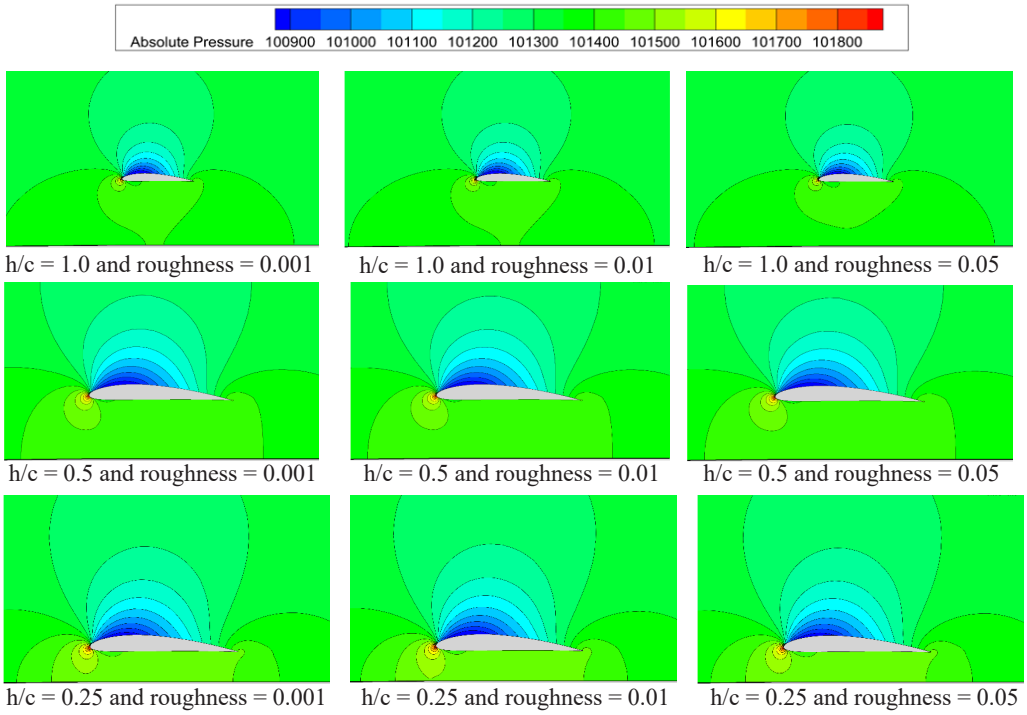

Figure 6. Pressure contour at 30 m/s

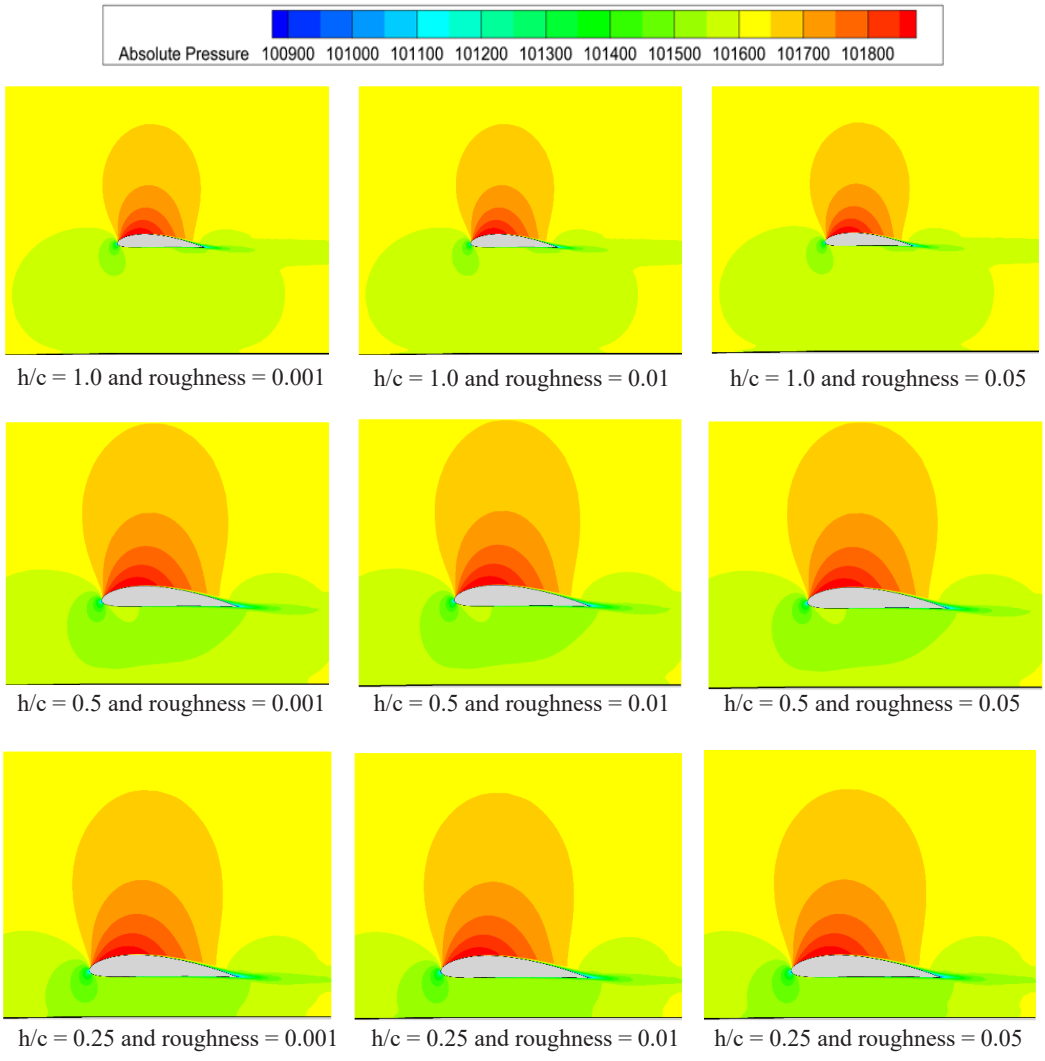

Figure 7. Velocity contour at 30m/s

RESULTS AND DISCUSSION

The results were obtained using the ANSYS package by giving the input values like velocity, surface roughness, and pressure in boundary conditions. As an output, we get the results like lift and drag coefficients for different AOA. The difference between pressure created above and below the body's surface when the body moves around in space and measuring this factor is known as the Lift coefficient. The drag coefficient is used to quantify the rearward force that disturbs the airflow of an airfoil and is a dimensionless quantity. The DATCOM results are obtained by inputting parameters like airfoil type, Reynolds number, Mach number, and angle of attack flight altitude. The CFD results for h/c = 0.4

and Reynolds number 3.2e5 are validated with the experimental results and compared with the DATCOM data. Figure 8 compares the lift coefficient obtained from Experimental, DATCOM, and CFD data. The plot shows that the computational results qualitatively agree with experimental values. However, the DATCOM data has discrepancies with the CFD and Experimental data. The DATCOM cannot predict the aerodynamic behavior of 4412 Airfoil with ground effects due to limitations in the code that the ground roughness cannot be given in the program.

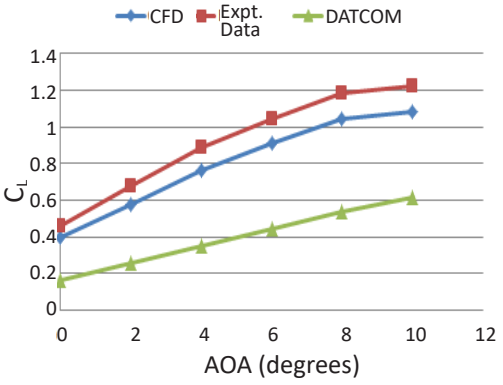

Figure 8. Lift coefficient vs. AOA for h/c = 0.4 and R_e= 3.2x10^5

Figure 9 depicts the NACA 4412 airfoil aerodynamic characteristics with ground effects for different roughness values with h/c as 1. The plot shows that the coefficient values vary from 0.4537 to 0.4571 and reach a maximum value at a roughness of 0.05, whereas the coefficient of drag varies from 0.0042 to 0.0055 and reaches a maximum value at a roughness of 0.001.

Figure 10 depicts the NACA 4412 airfoil aerodynamic characteristics for ground effects having different roughness values with h/c as 0.5. The plot shows that the coefficient values vary from 0.3558 to 0.356 and reach a maximum value at a roughness of 0.05, whereas the coefficient of drag varies from 0.0056 to 0.0196 and reaches a maximum value at a roughness of 0.001.

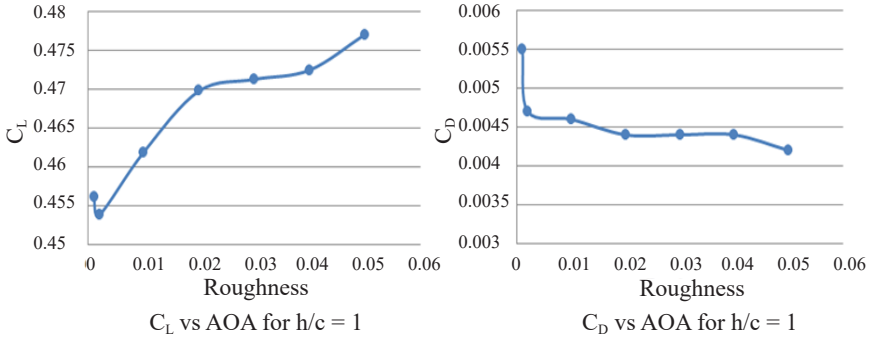

Figure 9. Aerodynamic characteristics for various roughness at h/c = 1

Figure 11 depicts the aerodynamic characteristics of the chosen airfoil with ground effects for different roughness values with h/c as 0.25. The plot shows that the coefficient values vary from 0.3398 to 0.4079 and reach a maximum value at a roughness of 0.05, whereas the coefficient of drag varies from 0.0071 to 0.0212 and reaches a maximum value at a roughness of 0.001.

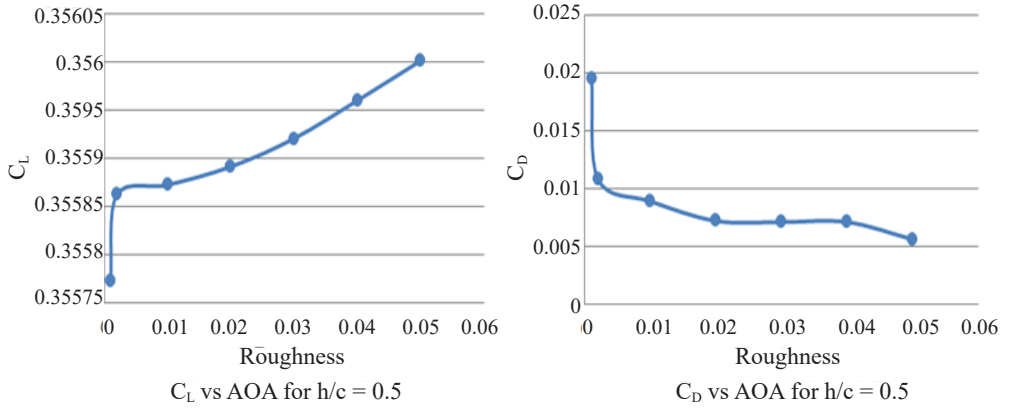

Figure 10. Aerodynamic characteristics for various roughness at h/c = 0.5

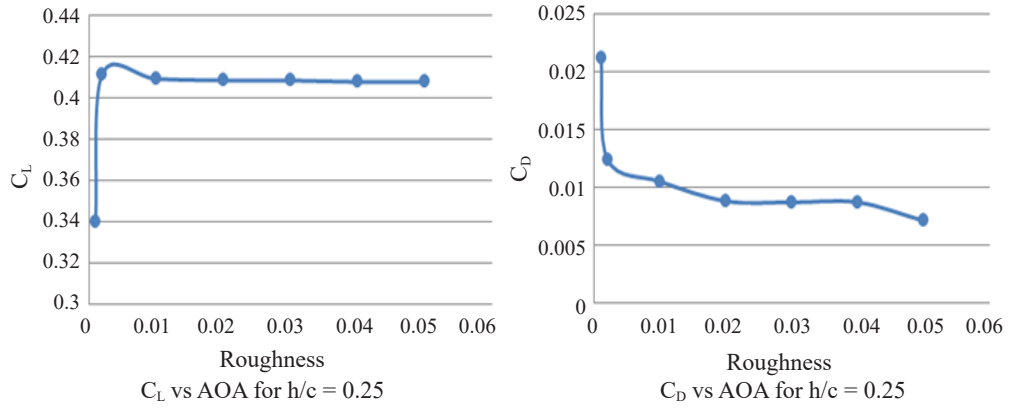

Figure 11. Aerodynamic characteristics for various roughness at h/c = 0.25

CONCLUSION

The present research examined airfoil flow physics and erodynamic characteristics (NACA 4412) by considering the ground effect for different h/c and surface roughness conditions. DATCOM prediction code cannot be used to predict aerodynamic characteristics with ground effects. The results show that the drag coefficient for different h/c ratios varies with a pattern, but the coefficient of lift does not follow any pattern. The coefficient of lift is at its highest value at a roughness of 0.05, while the coefficient of drag is at its lowest value at that same roughness, irrespective of the h/c ratio. In contrast, the coefficient of drag has a maximum value at a roughness of 0.001, whereas the coefficient of lift attains its maximum value at a roughness of 0.001 regardless of the h/c ratio. The difference between the max and min values is almost identical for the drag coefficient for diverse

h/c values. The results show that the roughness method implemented numerically in the present work shows some effects on the aerodynamic coefficients. However, it is not very significant, and the implementation of ground roughness physically is essential. Further future research can be continued by involving the wavy ground effects, which give the aerodynamic performance of the airfoil in real situations.

ACKNOWLEDGEMENT

This work is funded by ACSCE (Bangalore) and Raydynamics (Coimbatore), India.

REFERENCES

Abney, E., & McDaniel, M. (2005). High angle of attack aerodynamic predictions using missile datcom. In *23rd AIAA Applied Aerodynamics Conference* (p. 5086). AIAA. https://doi.org/10.2514/6.2005-5086

de Divitiis, N. (2005). Performance and stability of a winged vehicle in ground effect. *Journal of Aircraft*, *42*(1), 148-157. https://doi.org/10.2514/1.4830

Gao, B., Qu, Q., & Agarwal, R. K. (2018). Aerodynamics of a transonic airfoil in ground effect. *Journal of Aircraft*, *55*(6), *2240-2255.* https://doi.org/10.2514/1.C034998

Jamei., S., Maimun, A., Mansor, S., Azwadi, N., & Priyanto, A. (2012). Numerical investigation on aerodynamic characteristics of a compound wing-in-ground effect. *Journal of Aircraft*, *49*(5), 1297-1305. https://doi.org/10.2514/1.C031627

Kefalas, P., & Margaris, D. P. (2018). Aerodynamic analysis of a light aircraft using computational fluid dynamics. In *8th International Conference from Scientific Computing to Computational Engineering.* LFME.

Othman, N. (2017). Prediction of aerodynamic derivatives using Computational Fluid Dynamics (CFD) at transonic speed. *Journal of Transport System Engineering*, *4*(1), 8-16. https://jtse.utm.my/index.php/jtse/article/view/84

Page, G. J., & McGuirk, J. J. (2009). Large Eddy Simulation of a complete harrier aircraft in ground effect. *The Aeronautical Journal*, *113*(1140), 99-106. https://doi.org/ 10.1017/S0001924000002827

Papadopoulos, C., Mitridis, D., & Yakinthos, K. (2021). Conceptual design of a novel unmanned ground effect vehicle. In *IOP Conference Series, Materials Science and Engineering,* (Vol. 1024, No. 1, p. 012058). IOP Publishing. https://doi.org/10.1088/1757-899X/1024/1/012058

Paul, J. L., Vasile, J. D., & DeSpirito, J. (2021). Comparison of aeroprediction methods for guided munitions. In *AIAA 2021Forum* (p. 0024). AIAA. https://doi.org/10.2514/6.2021-0024

Qu, Q., Jia, X., Wang, W., Liu, P., & Agarwal, A. K. (2014a*).* Numerical simulation of the flowfield of an airfoil in dynamic ground effect. *Journal of Aircraft*, *51*(5), 1659-1662. https://doi.org/10.2514/1.C032452

Qu, Q., Lu, Z., Liu, P., & Agarwal, A. K. (2014b). Numerical study of aerodynamics of a wing-in-ground-effect craft. *Journal of Aircraft*, *51*(3), 913-924. https://doi.org/10.2514/1.C032531

Ramshankar, P., Sashikkumar, M., Ganeshan, P., & Raja, K. (2023). Experimental investigation of hybrid composites using biowastes and *Calotropis gigantea*: An eco-friendly approach. *Global NEST Journal, 25*(4)*,* 70-76. https://doi.org/10.30955/gnj.004620

Roozitalab, E., & Kharati-Koopaee, M. (2021). Effect of Gurney Flap on the aerodynamic behavior of an airfoil in mutational ground effect. *Proceedings of the Institution of Mechanical Engineers, Part G, Journal of Aerospace Engineering*, *235*(3), 339-355. https://doi.org/10.1177/0954410020943754

Sharma, A., Padthe, A., & Friedmann, P. P. (2021). Helicopter shipboard landing simulation including wind, deck motion and dynamic ground effect. *Journal of Aircraft*, *58*(3), 467-486. https://doi.org/10.2514/1.C035973

Vinayagar, K., Ganeshan, P., Raja, P. N., Hussain, M. S. Z., Kumar, P. V., Ramshankar, P., Mohanavel, V, Mathankumar, N., Raja, K., & Bezabih, T. T. (2022). Optimization of crashworthiness parameters of thin-walled conoidal structures. *Advances in Materials Science and Engineering*, *Article ID 4475605*. https://doi.org/10.1155/2022/4475605

Zheng, Y., Qu, Q., Liu, P., Wen, X., & Zhang, Z. (2021). Numerical analysis of the porpoising motion of a blended wing body aircraft during ditching. *Aerospace Science and Technology*, *119,* 107131. https://doi.org/10.1016/j.ast.2021.107131